A Modeling of Sphere Considering Slipping Adapted Three-Rollers

Kenji Kimura
Department of Control Engineering, National Institute of Technology, Matsue College
14-4 Nishi-ikuma-cho, Matsue-shi,Shimane,690-8518, Japan
*E-mail: k-kimura@matsue-ct.jp**

Kouki Ogata
Department of Physic, Faculty of Science and Engineering, Saga University
1 Honjo, Saga 840-8421, Saga, Japan
E-mail: ikokatago@gmail.com

Hiroyasu Hirai
Graduate School of Life Science and engineering, Kyushu Institute of Technology
2-4 Hibikino,Wakamatsu-ku, Kitakyushu-shi 808-0196, Fukuoka, Japan
E-mail: multipletitan@gmail.com

Takumi Ueda
Graduate School of Life Science and engineering, Kyushu Institute of Technology
2-4 Hibikino,Wakamatsu-ku, Kitakyushu-shi 808-0196, Fukuoka, Japan
E-mail: ueda@brain.kyutech.ac.jp

Kazuo Ishii
Graduate School of Life Science and engineering, Kyushu Institute of Technology
2-4 Hibikino,Wakamatsu-ku, Kitakyushu-shi 808-0196, Fukuoka, Japan
E-mail: ishii@brain.kyutech.ac.jp

Abstract

Many types of spherical robots use friction-drive systems for locomotion because such systems enable omnidirectional movement and are more capable of climbing steps than mobile robots equipped with multiple omni-wheels. Slipping between spheres and rollers is a remarkable issue with friction-driven mechanisms. However, the previously established sphere kinematic models do not consider slipping, and kinematic models consider slipping in only two constraint rollers. In this study, we propose a mathematical model that allows for slipping on three constraint rollers and simulate the angular velocity vector of the sphere and slip speed at each contact point.

Keywords: Angular velocity vector of the sphere, Motion analysis of the sphere, Slip velocity of the sphere

1. Introduction

A sphere is one of the main shapes of a robot. It is used not only as a multifingered fingertip mechanism for hand robots but also as an actuator transmission mechanism for omnidirectional movement and drive in mobile robots. Spheres are also used as driving rollers for omnidirectional movement mechanisms, with various arrangements and sphere structures depending on the application of the movement mechanism. **Figure 1** shows the roller contact type for the number of actuators ($\boldsymbol{N_R}$) per sphere.

In the case of $N_R = 2$, ACROBAT-S [1], wheel chair [2] have sphere kinematics (**Figures 1**(a) and (b)). The omnidirectional condition is that the rollers are arranged on the equator of the sphere[3]. Furthermore, the angular velocity vector of the sphere has two degrees of freedom. Theoretically, it is considered in [4].

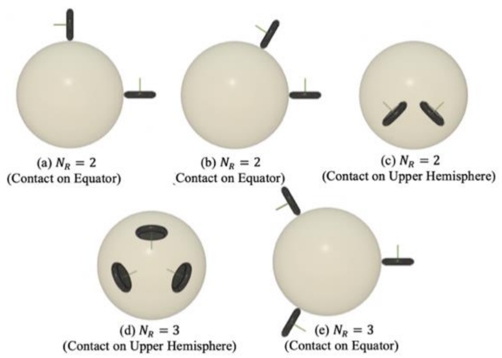

Figure 1 Type of roller arrangement for sphere mobile robot

As shown in **Figure 1**(c), the ball-holding mechanism [5] is designed to transport the ball. All robots in the RoboCup middle-size league (MSL) use a ball-dribbling mechanism to control the rotation of the ball, which is implemented with two rollers on the upper half of the ball. Most designs employ slip-roller arrangements, which are determined heuristically in experiments in the absence of suitable mathematical models because of their strong friction force and enhanced ball-holding ability. Here, the roller is arranged in the upper hemisphere with a slip at the contact point between the roller and the sphere.

In a previous study, we used two constraint rollers that allow for slipping to derive a mathematical model of sphere rotational motion [6]. This model is included in the kinematics of [4]. Furthermore, we employed experiment [7] to validate the model of [6].

In the case of $N_R = 3$, omnidirectional wheeled mobile platform (OWMP) [8] has three constraint rollers and a ball-balanced robot [9] has three unconstraint rollers (**Figures 1**(d)). The sphere rotational dimensions are different because of the roller structure. Each constrained roller has less rotational diversity than the unconstrained rollers. However, the holding force is stronger than that of the unconstrained roller. The stability of the sphere is higher in the case of three rollers than in the case of two rollers.

OWMP [8] is kinematic with a roller arrangement restricted to the equator; we extend this to an arbitrary arrangement discussion.

In this study, we modify the previously developed kinematic model [6] in the case of three constraint rollers and present a mathematical model of sphere rotational motion.

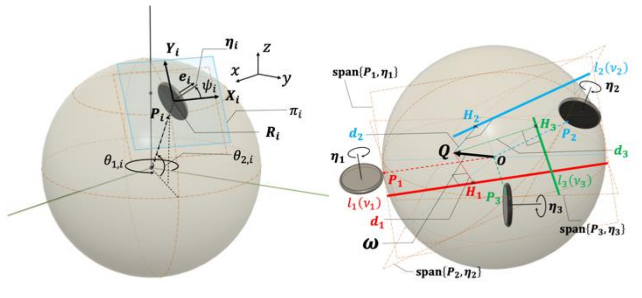

(a) (b)

Figure 2 (a). Roller axis vector $\boldsymbol{\eta_i}$ at contact point $\boldsymbol{P_i}$ on the sphere. (b). The existence of sphere angler velocity vector i

2. The sphere forward kinematics by three constraint rollers

In this section, we derive the angular velocity vector of the sphere to geometrically model.

2. 1 *The existence of angular velocity vector of the Sphere*

As shown in **Figure 2**(a), the center $\boldsymbol{O}$ of a sphere with radius r is fixed as the origin of the coordinate system $\Sigma - xyz$. The *i-th* constraint roller have mass $\boldsymbol{R_i}$ and contact point $\boldsymbol{P_i}$ with respect to sphere.

$\boldsymbol{\eta_i}$ denotes the unit vector along the rotational axis of the constraint roller. it has a starting point at $\boldsymbol{R_i}$ ($\boldsymbol{O}$, $\boldsymbol{P_i}$ and $\boldsymbol{R_i}$ are on the same line). $\boldsymbol{\omega}$ denotes the angular velocity vector of the sphere. ν_i denotes the peripheral speed of the constraint roller. The velocity vector of the sphere $\boldsymbol{\mathcal{V}_i^S}$ at $\boldsymbol{P_i}$ can be represented as $\boldsymbol{\mathcal{V}_i^S} = \boldsymbol{\omega} \times \boldsymbol{P}_i$. And $\boldsymbol{\mathcal{V}_i^R}$ denotes velocity vector of the roller. $\boldsymbol{e_i} \in \mathbf{span}\{\boldsymbol{P_i}, \boldsymbol{\eta_i}\}$ denotes unit normal vector along $\boldsymbol{\mathcal{V}_i^R}$. $\boldsymbol{e_i}$ and $\boldsymbol{\mathcal{V}_i^R}$ are satisfy $\nu_i = \langle \boldsymbol{\mathcal{V}_i^R}, \boldsymbol{e_i} \rangle$ ($\boldsymbol{\mathcal{V}_i^S} = \boldsymbol{\mathcal{V}_i^R}$: nonslip condition) Thus, $\boldsymbol{\omega}$ can be satisfied as follow.

$$\langle \boldsymbol{\eta_i}, \boldsymbol{\omega} \rangle = -\frac{\nu_i}{r} \tag{1}$$

$\boldsymbol{\omega}$ must be on $\mathbf{span}\{\boldsymbol{\eta_i}, \boldsymbol{P_i}\}$ and can be represented as a following line $l_i(\nu_i)$ that is parallel to $\boldsymbol{P_i}$ and passes through the end point of $-(\nu_i/r)\boldsymbol{\eta}_i$.

$$l_i(\nu_i) = \left\{\boldsymbol{\omega} \middle| \left(-\frac{\nu_i}{r}\right)\boldsymbol{\eta}_i + t(1/r)\boldsymbol{P}_i, t \in \mathbb{R}\right\} \tag{2}$$

$\boldsymbol{R_i}$ is located along the plane π_i parallel to the tangent plane of the sphere at $\boldsymbol{P_i}$ (polar coordinate). We put vectors as normal orthogonal base $\{\boldsymbol{X_i}, \boldsymbol{Y_i}\}$ on π_i at start point $\boldsymbol{R_i}$. Thus, $\boldsymbol{\eta_i}$ is linear combination of Eq. (6) and rotates counterclockwise with respect to ψ_i.

$$\boldsymbol{\eta_i} = [\, \boldsymbol{X_i} \cos\psi_i + \boldsymbol{Y_i} \sin\psi_i] \tag{3}$$

Where

$$\boldsymbol{X_i} = \begin{bmatrix} -\sin\theta_{1,i} \\ \cos\theta_{1,i} \\ 0 \end{bmatrix}, \ \boldsymbol{Y_i} = \begin{bmatrix} -\sin\theta_{2,i}\cos\theta_{1,i} \\ -\sin\theta_{2,i}\sin\theta_{1,i} \\ \cos\theta_{2,i} \end{bmatrix} \quad (4)$$

2.2 Calculation *of Optimal point in sum of the squared distances*

we calculate the optimal point $\boldsymbol{Q_o} = (x_0, y_0, z_0)(\in \mathbb{R}^3)$, which is determined such that the sum of the squared distances between $\boldsymbol{Q} = (x, y, z)(\in \mathbb{R}^3)$ and $l_i(v_i)(i = 1, 2, 3)$ is minimized.

As shown in **Figure 2**(b), the distances between $\boldsymbol{Q}$ and $l_i(v_i)$ in each line $l_i(v_i)$ is represented. Therefore, the sum of the squared distances is represented as follow:

$$L(x, y, z) = {d_1}^2 + {d_2}^2 + {d_3}^2 \quad (5)$$

where

$$d_i = \left\| \left(-\frac{v_i}{r}\right)\boldsymbol{\eta}_i + \frac{\langle \boldsymbol{P}_i, \boldsymbol{Q} \rangle}{r^2}\boldsymbol{P}_i - \boldsymbol{Q} \right\| \quad (6)$$

$(x, y, z) = (x_0, y_0, z_0)$ such that $L(x, y, z)$ is minimal value is satisfy as following.

$$z_0 = -\frac{E_9}{2E_3}, y_0 = \frac{D_5E_9 - 2D_8E_3}{4D_2E_3}$$
$$x_0 = \frac{1}{8C_1D_2E_3}(-C_4D_5E_9 + 2C_4D_8E_3 + 2C_6D_2E_9 - 4D_2E_3C_7) \quad (7)$$

Where

$$E_3 = D_3 - \frac{{D_5}^2}{4D_2}, E_9 = D_9 - \frac{D_5D_8}{2D_2}, E_{10} = D_{10} - \frac{{D_8}^2}{4D_2} \quad (8)$$

Where

$$D_2 = C_2 - \frac{{C_4}^2}{4C_1}, D_3 = C_3 - \frac{{C_6}^2}{4C_1}, D_5 = C_5 - \frac{C_4C_6}{2C_1}$$
$$D_8 = C_8 - \frac{C_4C_7}{2C_1}, D_9 = C_9 - \frac{C_6C_7}{2C_1}, D_{10} = C_{10} - \frac{{C_7}^2}{4C_1}$$

(9)

Where

$$C_{10} = L(0,0,0)$$
$$C_1 = \frac{1}{2}\big(L(1,0,0) + L(-1,0,0) - 2L(0,0,0)\big)$$
$$C_2 = \frac{1}{2}\big(L(0,1,0) + L(0,-1,0) - 2L(0,0,0)\big)$$
$$C_3 = \frac{1}{2}\big(L(0,0,1) + L(0,0,-1) - 2L(0,0,0)\big)$$
$$C_7 = \frac{1}{2}\big(L(1,0,0) - L(-1,0,0)\big)$$
$$C_8 = \frac{1}{2}\big(L(0,1,0) - L(0,-1,0)\big)$$
$$C_9 = \frac{1}{2}\big(L(0,0,1) - L(0,0,-1)\big) \quad (10)$$
$$C_4 = \frac{1}{4}\big(L(1,1,0) - L(-1,1,0) - L(1,-1,0) + L(-1,-1,0)\big)$$
$$C_5 = \frac{1}{4}\big(L(0,1,1) - L(0,-1,1) - L(0,1,-1) + L(0,-1,-1)\big)$$
$$C_6 = \frac{1}{4}\big(L(1,0,1) - L(1,0,-1) - L(-1,0,1) + L(-1,0,-1)\big)$$

3. Simulation

This section presents the simulation results, including the trajectory of the endpoint of the angler velocity vector $\boldsymbol{\omega}_k$ and slip speed of sphere and roller $\|\boldsymbol{\zeta}_k\|$ in *k-th* pattern of roller arrangement ($k = 1,2,3,4$) in the case in which a regular triangle ($\theta_{1,1}$, $\theta_{1,2}$, $\theta_{1,3}$) $= (30°, 150°, 270°)$and $\psi_i = 0°(i = 1,2,3,4)$. The patterns are set up by $\theta_{2,i}$ $(i = 1,2,3,4)$ as follows: Pattern I ($k = 1, \theta_{2,i} = 0°$), Pattern II ($k = 2, \theta_{2,i} = 10°$), Pattern III ($k = 3, \theta_{2,i} = 20°$), Pattern IV ($k = 4, \theta_{2,i} = 30°$).

As input, we define function $v_1(\varphi) = \sin(\varphi + 240°)$,$v_2(\varphi) = \sin(\varphi + 120°)$ and$v_3(\varphi) = \sin\varphi$.

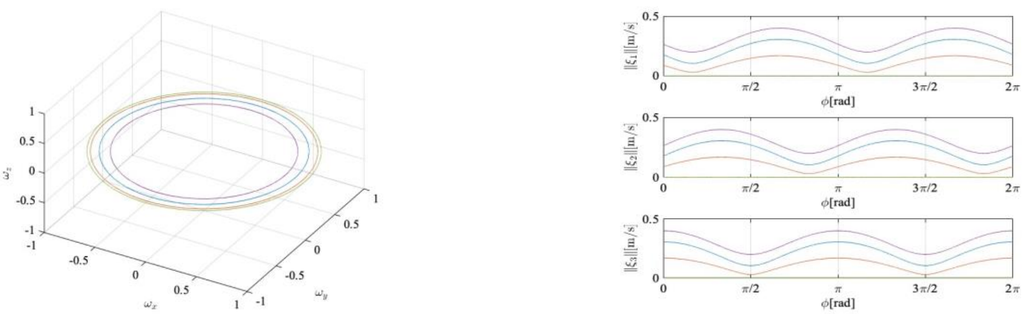

(a) (b)

Figure 3 Simulation and comparisons in *k-th* pattern of roller arrangement ($k = 1,2,3,4$) (a). Trajectory of end point of angular velocity vector $\boldsymbol{\omega}_k$ (b). Slip speed of sphere and roller $\|\boldsymbol{\zeta}_{1,k}\|$, $\|\boldsymbol{\zeta}_{2,k}\|$, $\|\boldsymbol{\zeta}_{3,k}\|$.

As output, $\boldsymbol{\omega}_k$ and $\|\boldsymbol{\zeta}_k\|$ $(k = 1,2,3,4)$ were indicated, such as Pattern I [$k = 1$; green curve], Pattern II [$k = 2$; red curve], Pattern III [$k = 3$; blue curve], and Pattern IV [$k = 4$; violet curve] (**Figure 3**).

As shown in **Figure 3**(a), $\boldsymbol{\omega}_k$ $(k = 1,2,3,4)$ draws circle trajectories and gets a small radius in turn.

As shown in **Figure 3**(b), duo to Pattern I (nonslip case), $\|\boldsymbol{\zeta}_{1,1}\|$, $\|\boldsymbol{\zeta}_{2,1}\|$, and $\|\boldsymbol{\zeta}_{3,1}\| = 0$ [m/s]. $\|\boldsymbol{\zeta}_{1,k}\|$, $\|\boldsymbol{\zeta}_{2,k}\|$, $\|\boldsymbol{\zeta}_{3,k}\|$ have minimal values of 0.03, 0.10, and 0.19 [m/s] and maximal values of 0.16, 0.30, and 0.40 [m/s], respectively.

4. Conclusion

In this study, we considered the existence of an angular velocity vector for the sphere and proposed a sphere forward kinematics model that allows for slipping. Furthermore, we demonstrated the trajectory of the endpoint of the angler velocity vector and behavior of slip speed. and obtained maximal and minimal values.

In future research, this model will be verified experimentally. It could also be applied to a mobile robot.

Reference

[1] M.Wada, K.Kato, "Kinematic modeling and simulation of active-caster robotic drive with a ball transmission (ACROBAT-S)". 2016 IEEE/RSJ International Conference on Intelligent Robots and Systems. Daejeon, 2016-12-9/25, IEEE Robotics and Automation Society,

[2] S.Ishida , H.Miyamoto,"Holonomic Omnidirectional Vehicle with Ball Wheel Drive Mechanism, 2012 The Japan Society of Mechanical Engineers.Vol.78,No.790, pp.2162-2170, 2012.

[3] K. Kimura, K. Ishii, Y. Takemura, M. Yamamoto, Mathematical Modeling and motion analysis of the wheel based ball retaining mechanism, *SCIS & ISIS*, pp.4106-4111, 2016.

[4] K. Kimura, S. Chikushi, et al, Motion Analysis of a Sphere Driven by Rollers, Journal of the Robotics Society of Japan. Vol.38, No.5, pp.485-495, 2020.

[5] S. Chikushi, M. Kuwada, et al., Development of Next-Generation Soccer Robot"Musashi150"for RoboCup MSL,*30th Fussy System Symposium*, pp. 624-627,2014.

[6] K. Kimura, K. Ogata, K. Ishii, Novel Mathematical Modeling and Motion Analysis of a Sphere Considering Slipping, Journal of Robotics, Networking and Artificial Life, Vol.6, issue 1, pp. 27-32, 2019.

[7] K. Kimura, S. Chikushi, K. Ishii, Evaluation of the Roller Arrangements for the Ball-Dribbling Mechanisms adopted by RoboCup Teams, Journal of Robotics, Nrtworking and Artificial Life, Vol.6, issue 3, pp. 183- 190, 2019.

[8] M. Kumagai, T. Ochiai: "Development of a robot balanced on a ball – Application of passive motion to transport",Proc. ICRA IEEE(2009), pp. 4106-4111, 2009.

[9] Lee,Y.C,Danny,Lee,D.V.,Chung,J.,andVelinky,S.A.,"Control of a redundant, reconfigurable ball wheel drive mechanism for an omunidirectional platform",Robotica, Cambridge University Press,Vol.25, pp.385-395, 2007.

Authors Introduction

Dr. Kenji Kimura

He is a Lecturer in Department of Control Engineering, National Institute of Technology, Matsue College, He received his ME (mathematics) from Kyushu University in 2002 and received his Ph.D. degree in engineering from Kyushu Institute of Technology in 2020.

Mr. Kouki Ogata

He received education in Fukuoka Daiichi high school until 2016, He is currently undergraduate School student at Saga University. His current research interests include sphere mobile robot kinematics, analytical dynamics.

Mr. Hiroyasu Hirai

He received his B.E. and M.E., in Computer Science from Nippon Bunri University, Japan, in 2013 and 2016, respectively. He is a 3rd year student in the doctoral program of the Kyushu Institute of Technology.

Mr. Takumi Ueda

He received his M.E., in Engineering from Kyusyu Institute of Technology, Japan, in 2017. He is a 3rd year student in the doctoral program of the Kyushu Institute of Technology. His research interest includes non-linear control by PID using database.

Dr. Kazuo Ishii

He is a Professor in the Kyushu Institute of Technology. He received his Ph.D. degree in engineering from University of Tokyo, in 1996. His research interests span ship marine engineering and Intelligent Mechanics.